Reconfiguration of a Rolling Sphere: A Problem in Evolute-Involute Geometry

Tuhin Das

Ranjan Mukherjee
Associate Professor
e-mail: mukherji@egr.msu.edu

Department of Mechanical Engineering,
Michigan State University,
East Lansing, MI 48824

This paper provides a new perspective to the problem of reconfiguration of a rolling sphere. It is shown that the motion of a rolling sphere can be characterized by evolute-involute geometry. This characterization, which is a manifestation of our specific selection of Euler angle coordinates and choice of angular velocities in a rotating coordinate frame, allows us to recast the three-dimensional kinematics problem as a problem in planar geometry. This, in turn, allows a variety of optimization problems to be defined and admits infinite solution trajectories. It is shown that logarithmic spirals form a class of solution trajectories and they result in exponential convergence of the configuration variables. [DOI: 10.1115/1.2164515]

1 Introduction

The rolling sphere epitomizes the complexity of diverse problems in mechanics involving geometry of rotations and its reconfiguration has similarities with many engineering problems, such as spacecraft attitude reorientation and manipulation of rigid objects using robotic fingers. The configuration of a rolling sphere is described by two Cartesian coordinates of its center and three orientation coordinates, and reconfiguration refers to the task of designing a trajectory that enables it to roll from an arbitrary configuration to a desired configuration. This problem has seen a few solutions until date but new approaches and solutions to the problem should be welcome since they can provide new insight into the realm of rotational kinematics. In this paper, we show that the kinematics of a rolling sphere can be described by evolute-involute geometry and provide a fundamentally new approach towards solving the reconfiguration problem.

To the best of our knowledge, Hammersley [1] provided the first solution to the reconfiguration problem in 1983. A simpler solution to the problem in the form of a three-step algorithm was proposed by Li and Canny [2] in 1990. In the first step, the two Cartesian coordinates of the sphere are converged to their desired values. The second step generates an equatorial triangle on the surface of the sphere and converges two of the three orientation coordinates, and the third step uses a polhode to converge the third orientation coordinate. An optimal solution, based on minimization of integral of the kinetic energy of the sphere, was provided by Jurdjevic [3] in 1993. The results are elegant and indicate that the optimal trajectories are described by elliptic functions. In 2002, Mukherjee et al. [4] proposed two computationally efficient motion planning algorithms for the rolling sphere. The first algorithm is based on planar geometry whereas the second algorithm is based on spherical trigonometry.

In relation to the above papers, where the primary focus has been the solution to the reconfiguration problem, this paper establishes a fundamental property of the motion of rolling spheres, namely, the motion is equivalent to the action of wrapping and unwrapping a taut rope on a planar curve. This evolute-involute geometric characterization is a manifestation of our specific selection of Euler angle coordinates and choice of angular velocities in the rotating coordinate frame. The planar geometric formulation of the problem admits infinite solution trajectories and allows us to pose a variety of optimization problems with different objective functions, including the isoperimetric problem [5]. Clearly, the importance of the paper lies in the generality of the adopted approach rather than the specific solution to the problem provided on the basis of the approach.

In search of a class of solution trajectories for the sphere motion planning problem, discussed above, we investigate the Sweep-Tuck algorithm [6] which provides the first and only solution to the feedback stabilization problem. For our open-loop geometric problem, we show that the nonsmooth trajectories provided by the Sweep-Tuck algorithm transform into a class of smooth solution trajectories under limiting conditions. These solution trajectories form an evolute-involute pair of logarithmic spirals and result in exponential convergence of the configuration variables.

This paper is organized as follows: In Sec. 2 we present the kinematic model of the rolling sphere and give an overview of the Sweep-Tuck algorithm. In Sec. 3 we describe the motion of the sphere using evolute-involute geometry and pose the reconfiguration problem. In Sec. 4, we present an algorithm for partial reconfiguration of the sphere. The flexibility of the partial reconfiguration algorithm is exploited in developing the complete reconfiguration algorithm in Sec. 5. In Sec. 6 we present simulation results and concluding remarks are presented in Sec. 7.

2 Background

2.1 Kinematic Model. Consider an arbitrary configuration of the sphere, as shown in Fig. 1(*a*). We denote the Cartesian coordinates of the sphere center by $Q \equiv (x, y)$ and adopt the z-y-z Euler angle sequence (α, θ, ϕ) to represent the orientation of the sphere. As per the z-y-z Euler angle sequence, the inertially fixed xyz frame is first rotated about the positive z axis by angle α, $-\pi \leqslant \alpha \leqslant \pi$, to obtain the frame $x_1y_1z_1$. The frame $x_1y_1z_1$ is then rotated about the y_1 axis by angle θ, $0 \leqslant \theta \leqslant \pi$, to obtain frame $x_2y_2z_2$. Finally, the $x_2y_2z_2$ frame is rotated about the z_2 axis by angle ϕ to obtain frame $x_3y_3z_3$, which is fixed to the sphere. The points P and R are defined to be the intersection points of the sphere surface with the z_3 and x_3 axes, respectively. Assuming the sphere to have unity radius without any loss of generality, and denoting the angular velocities of the sphere about the x_1, y_1, z_1 axes as ω_x^1, ω_y^1, ω_z^1, respectively, the state equations for $\omega_z^1 = 0$ (the assumption $\omega_z^1 = 0$ is made to impose the constraint that the sphere cannot spin about the vertical axis) can be written as follows [4]:

Contributed by the Applied Mechanics Division of ASME for publication in the JOURNAL OF APPLIED MECHANICS. Manuscript received February 23, 2005; final manuscript received October 28, 2005. Review conducted by N. Sri Namachchivaya. Discussion on the paper should be addressed to the Editor, Prof. Robert M. McMeeking, Journal of Applied Mechanics, Department of Mechanical and Environmental Engineering, University of California-Santa Barbara, Santa Barbara, CA 93106-5070, and will be accepted until four months after final publication in the paper itself in the ASME JOURNAL OF APPLIED MECHANICS.

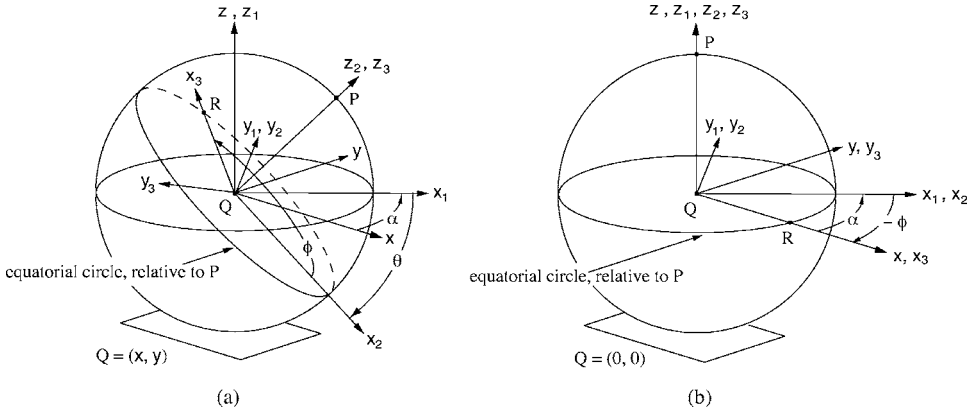

Fig. 1 (***a***) **An arbitrary configuration of the sphere;** (***b***) **desired configuration of the sphere**

$$\dot{x} = \omega_y^1 \cos\alpha + \omega_x^1 \sin\alpha \tag{1}$$

$$\dot{y} = \omega_y^1 \sin\alpha - \omega_x^1 \cos\alpha \tag{2}$$

$$\dot{\theta} = \omega_y^1 \tag{3}$$

$$\dot{\alpha} = -\omega_x^1 \cot\theta \tag{4}$$

$$\dot{\beta} = \omega_x^1 \tan(\theta/2) \tag{5}$$

where β is defined as follows:

$$\beta = \alpha + \phi \tag{6}$$

The reorientation of the sphere refers to the task of bringing P to the vertically upright position, and R, which then lies on the diametrical circle in the xy plane, to lie on the positive x axis. This can be achieved with $\theta=0$ and $\beta=0$, irrespective of the individual values of α and ϕ, as shown in Fig. 1(*b*). This is related to the notion of controllability and elaborated in [4]. Therefore, the sphere can be completely reconfigured by designing trajectories for ω_x^1 and ω_y^1 that result in

$$x=0, \quad y=0, \quad \theta=0, \quad \alpha+\phi=\beta=0 \tag{7}$$

2.2 Effect of Rotations About Moving Coordinates. Consider the motion of the sphere for the following actuations:

(A) $\omega_y^1 \neq 0,\ \omega_x^1 = 0$
(B) $\omega_x^1 \neq 0,\ \omega_y^1 = 0,\ \theta \neq 0$

The motion of the sphere for these actions is explained with the help of Fig. 2. Under action (A), the sphere moves along straight line CF as θ changes. Let F be the point on this straight line where the sphere would have $\theta=0$. Since the sphere rolls without slipping, this point remains invariant under action (A). For actuation (B), the instantaneous radius of the path traced by the sphere on the xy plane can be computed using Eqs. (1)–(4) as follows:

$$\rho = \left| \frac{(\dot{x}^2 + \dot{y}^2)^{3/2}}{\dot{x}\ddot{y} - \dot{y}\ddot{x}} \right| = \tan\theta \tag{8}$$

Since $\omega_y^1=0$, θ is maintained constant. This implies that the contact point of the sphere, the center of the sphere, and points P and F move in the horizontal plane along circular arcs whose center lie on the vertical axis that passes through C. We can easily show that distance CF satisfies

$$CF = \tan\theta - \theta \tag{9}$$

The point C remains fixed under actuation (B), but under actuation (A) moves away from F, as θ increases, and converges to F, as θ converges to zero. The variables α and β in Eqs. (4) and (5) change during actuation (B) but remain constant during actuation (A). During actuation (B), the change in variable β is given by the expression

$$\Delta\beta = \Delta\alpha + \Delta\phi = \Delta\alpha(1 - \sec\theta) \tag{10}$$

2.3 Partial Reconfiguration Using the Sweep-Tuck Algorithm. In this section we present the main results of the Sweep-Tuck algorithm detailed in [6]. With reference to Fig. 1, we define partial reconfiguration as the task of converging Q to the origin of the Cartesian coordinate frame and P to the vertically top position. This allows R to have an arbitrary location on the equatorial circle but requires us to satisfy

$$x=0, \quad y=0, \quad \theta=0 \tag{11}$$

Now consider an arbitrary configuration of the sphere as shown in Fig. 3. The points C and F in Fig. 3 were defined earlier in Sec. 2.2 using Fig. 2. It can be shown that

$$(CF, CO) \equiv (0,0) \Leftrightarrow (x, y, \theta) \equiv (0,0,0) \tag{12}$$

and this motivates the following remark:

Remark 1. The sphere in Fig. 3 will be partially reconfigured in the sense of Eq. (11) if and only if (CF, CO) *converge to* (0,0).

Towards the goal of partial reconfiguration, we now recall the following theorem from [6].

DUAL-POINT THEOREM. *Let C and F be two points in the xy plane with origin at O, as shown in Fig. 4. Suppose* $\psi = \angle OCF$ *is*

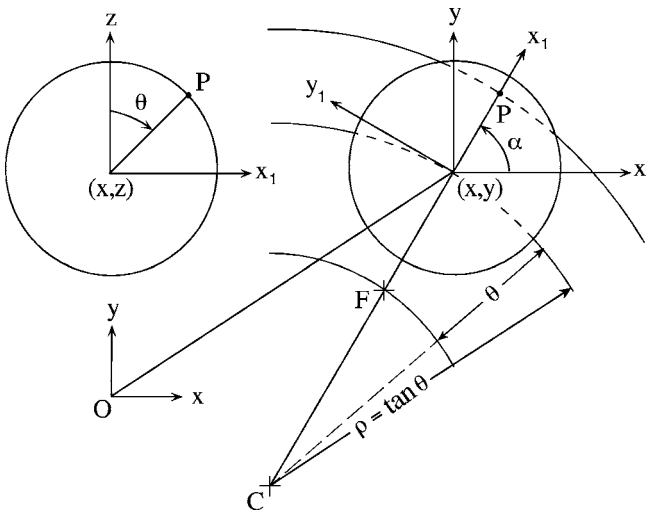

Fig. 2 Actuations (A) and (B)

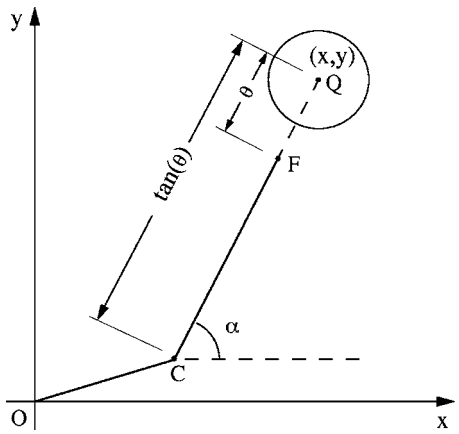

Fig. 3 An arbitrary configuration of the sphere

acute, and let $(CF/CO)=\lambda, \lambda \in (1,\infty)$. *If* ψ *satisfies the condition*

$$0 \leqslant \psi < \cos^{-1}(1/\lambda) \tag{13}$$

then there exists a point C' *on the extended line CF such that for* $\psi' = \angle OC'F$, $0 \leqslant \psi' \leqslant \pi$,

$$(C'F/C'O) = \lambda \cdots (i) \quad 0 < (C'O/CO) < 1 \cdots (ii)$$

$$\psi' > \psi \cdots (iii) \tag{14}$$

Remark 2. In [6] the Dual-Point Theorem is stated and proved for both cases $\lambda \in (1,\infty)$ and $\lambda \in (0,1)$. However, we restrict ourselves to the case $\lambda \in (1,\infty)$ in this paper.

The intermediate angle, ψ', can be expressed as follows [6]:

$$\tan\psi' = \frac{-|1-\lambda^2|\sin\psi}{(1+\lambda^2)\cos\psi - 2\lambda}, \quad \lambda \in (1,\infty) \tag{15}$$

and it can be shown that Eq. (13) implies

$$\cos^{-1}\left(\frac{1}{\lambda}\right) < \psi' \leqslant \pi \tag{16}$$

Now consider Fig. 5 where C and F define an arbitrary configuration of the sphere. Suppose $\psi = \angle OCF$ satisfies the conditions in Eq. (13). Let C' in Fig. 5 be the point on line CF that satisfies the conditions in Eq. (14). We now define three specific maneuvers of the sphere.

DEFINITION 1 (DPT MANEUVER). *A "Dual-Point Tuck" (DPT) Maneuver is an actuation (A) that moves the sphere such that C moves to* C'.

From Dual-Point Theorem we know that a DPT maneuver results in $\psi' > \psi$. Therefore, ψ' can be restored to the value ψ in one of two ways as shown in Fig. 5. This motivates the next definition.

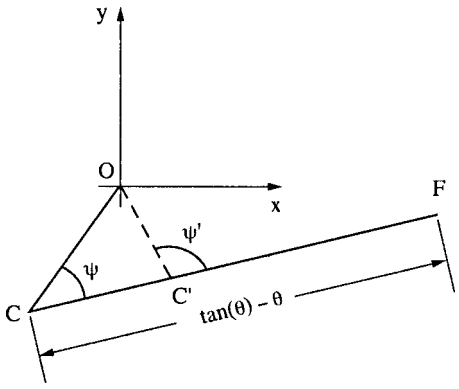

Fig. 4 The *C*-*C*′ pair for the Dual-Point Theorem

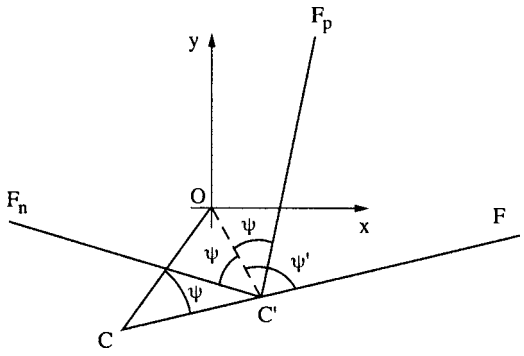

Fig. 5 RS and DPT maneuvers

DEFINITION 2 (RS MANEUVER). *Following a DPT maneuver, an actuation (B) that moves the sphere to restore* ψ' to ψ *is defined as a "Restoring-Sweep" (RS) Maneuver.*

DEFINITION 3 (PS MANEUVER). *An actuation (B) that moves the sphere at the initial time to bring* $\angle OCF$ *to* ψ' *is defined as a "Preliminary-Sweep" (PS) Maneuver.*

We now present the "Sweep-Tuck" algorithm [6].

Sweep-Tuck Algorithm. Consider a sphere whose partial configuration (x,y,θ), defined by the location of points C and F, initially satisfies $0 < \theta \leqslant (\pi/2 - \epsilon)$ and $(CF/CO) = \lambda \in (1,\infty)$. If ψ is chosen in accordance with Eq. (13), partial reconfiguration in the sense of Eq. (11) can be achieved through a PS maneuver followed by repeated application of RS-DPT maneuvers.

The Sweep-Tuck algorithm utilizes the fact that alternate RS and DPT maneuvers decrease both CF and CO in geometric progression; the rate at which CF and CO decrease depends on n and ψ [6]. The distance traversed by C during each DPT maneuver also depends on n and ψ and is given by the relation

$$CC' = \frac{2\lambda CO(\lambda\cos\psi - 1)}{(\lambda^2 - 1)} \tag{17}$$

3 Geometry of Reconfiguration

3.1 The Evolute-Involute Pair. We investigated the motion of C and F in Sec. 2.2, where the actuating inputs ω_x^1 and ω_y^1 were not applied simultaneously, i.e., $\omega_y^1 = 0$ when $\omega_x^1 \neq 0$, and vice versa. In this section we investigate the motion of C and F under simultaneous variation of ω_x^1 and ω_y^1. To this end we first note that the coordinates of C and F can be obtained from Fig. 3 as follows:

$$C_x = x - \tan\theta\cos\alpha \quad F_x = x - \theta\cos\alpha$$

$$C_y = y - \tan\theta\sin\alpha \quad F_y = y - \theta\sin\alpha \tag{18}$$

By differentiating the above equations and substituting Eqs. (1)–(5) we get

$$\dot{C}_x = -\omega_y^1\cos\alpha\tan^2\theta \quad \dot{F}_x = \omega_x^1\sin\alpha(1 - \theta\cot\theta)$$

$$\dot{C}_y = -\omega_y^1\sin\alpha\tan^2\theta \quad \dot{F}_y = -\omega_x^1\cos\alpha(1 - \theta\cot\theta) \tag{19}$$

From Eq. (19) we deduce

$$dC_y/dC_x = \tan\alpha \quad \text{for } \theta \neq 0 \text{ and } \omega_y^1 \neq 0$$

$$dF_y/dF_x = -\cot\alpha \quad \text{for } \theta \neq 0 \text{ and } \omega_x^1 \neq 0 \tag{20}$$

We note from Figs. 2 and 3 that the instantaneous slope of CF is $\tan\alpha$. This motivates the following remark.

Remark 3. Under simultaneous application of actuating inputs ω_x^1 and ω_y^1, the instantaneous motion of C and F are tangential and perpendicular, respectively, to line CF.

Remark 3 outlines the qualitative nature of the trajectory of F,

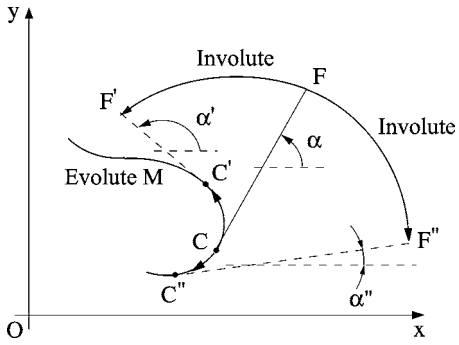

Fig. 6 Motion of *C* and *F* due to ω_x^1 and ω_y^1

given a trajectory of C. It indicates that if C is constrained to follow a desired curve, F will traverse a path such that for any instantaneous position of C, CF is tangential to the curve at that point. This is illustrated in Fig. 6 where C is constrained to follow the curve M. As C moves to C' or C'', F moves to F' or F'', respectively, such that $C'F'$ or $C''F''$ are tangential to the curve M at C' or C'', respectively. Using Eqs. (1)–(5) and (18), we can now show

$$\Delta C_x = -\cos\alpha \tan^2\theta \Delta\theta$$

$$\Delta C_y = -\sin\alpha \tan^2\theta \Delta\theta \tag{21}$$

which leads to

$$|\Delta C| = (\Delta C_x^2 + \Delta C_y^2)^{1/2} = \tan^2\theta |\Delta\theta| \tag{22}$$

Also, from Eq. (9) we obtain

$$CF = (\tan\theta - \theta) \Rightarrow |\Delta CF| = \tan^2\theta |\Delta\theta| \tag{23}$$

Equations (22) and (23) effectively imply that for an infinitesimal distance $\Delta\mathcal{L}_C$ traversed by C along its trajectory

$$|\Delta CF| = \Delta\mathcal{L}_C \tag{24}$$

Remark 3 and Eq. (24) together lead to the interesting geometric result that the distance traversed by C along its constrained trajectory M equals the change in length of CF. The result can be visualized with CF as a taut rope wrapping or unwrapping on a two-dimensional curve M. During wrapping or unwrapping, the rope always remains tangential to the curve, the point of contact being C and the other end being F as illustrated in Fig. 6. The action of wrapping is illustrated by the transition of C and F to C' and F', respectively, where distance $C'F' < CF$. Similarly, unwrapping is illustrated by the transition to C'' and F'', where distance $C''F'' > CF$. The observations made above immediately imply that the trajectories of C and F form a *Evolute-Involute* pair. The trajectory of F is an involute of the trajectory of C, which is the evolute. We summarize our observations in Remark 4 below.

Remark 4. If the point C is constrained to traverse a prescribed path by the inputs ω_x^1 and ω_y^1, the point F moves such that CF is tangential to the trajectory of *C and CF* "wraps" or "unwraps" on the curve followed by C. The trajectories of the points C and F form an Evolute-Involute pair.

The evolute and involute trajectories of points C and F provide a fundamentally new description of the motion of rolling spheres. This description is a direct manifestation of our specific selection of Euler angle coordinates and choice of angular velocities of the sphere in the rotating coordinate frame. In the next section we utilize the evolute-involute geometric description to pose the reconfiguration problem as a problem in planar geometry.

3.2 Geometry Based Problem Definition. For partial reconfiguration of the sphere, C and F must simultaneously converge to the origin—this follows from Remark 1. For a given trajectory of C, we infer from Sec. 3.1 that, to converge F simultaneously, the

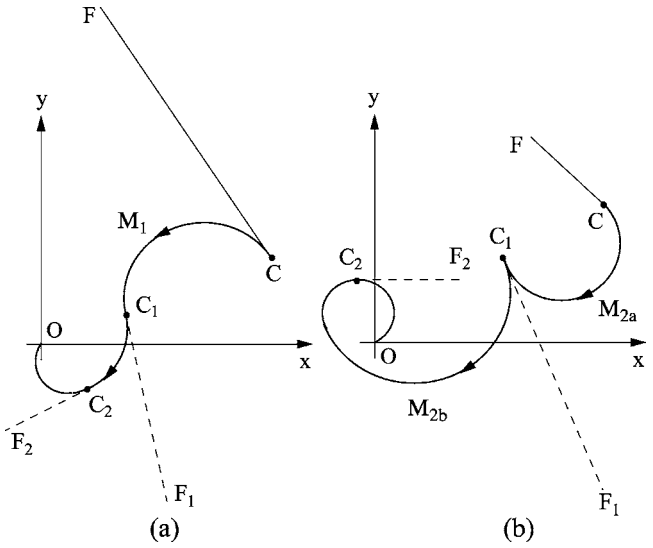

Fig. 7 Wrapping and unwrapping trajectories of the point *C*

length of the trajectory of C should be equal to the initial length of CF. This is illustrated in Fig. 7(*a*), where the length of the path M_1 equals CF and hence C and F simultaneously converge to the origin. It may be argued that this approach is not applicable when $CF \leqslant CO$. However, this is not true as illustrated in Fig. 7(*b*). Here, C first follows a path M_{2a} that unwraps CF so that $C_1F_1 > CF$. The subsequent path M_{2b} then wraps CF to converge both C and F simultaneously to the origin. Note that C_1F_1 is tangential to both the curves M_{2a} and M_{2b} at the point C_1. This is in accordance with the characteristics of the motion of C and F, established in Remark 4. We shall now classify the trajectories of C, i.e. the evolutes, into two different categories

DEFINITION 4. *A "wrapping" evolute is one where the length of CF decreases as C traverses the trajectory.*

Some examples of wrapping trajectories are M_1 and M_{2b} given in Figs. 7(*a*) and 7(*b*), respectively. Any arbitrary point on a wrapping trajectory satisfies the condition

$$\hat{u}_t \cdot \frac{\overrightarrow{CF}}{|\overrightarrow{CF}|} = +1$$

where $\hat{u}_t$ is the unit tangent vector to the evolute.

DEFINITION 5. *An "unwrapping" evolute is one where the length of CF increases as C traverses the trajectory.*

An example of an unwrapping trajectory is M_{2a} in Fig. 7(*b*). An arbitrary point on an unwrapping trajectory satisfies the condition

$$\hat{u}_t \cdot \frac{\overrightarrow{CF}}{|\overrightarrow{CF}|} = -1$$

Remark 5. For partial reconfiguration, the trajectory of C must consist of either a single wrapping evolute, as in Fig. 7(*a*), or a sequence of alternate unwrapping and wrapping evolutes, such as in Fig. 7(*b*). Furthermore, the wrapping and unwrapping evolutes should be designed such that

$$\sum_{i=1}^{n} \mathcal{L}[\mathcal{C}_{wi}] - \sum_{j=0}^{m} \mathcal{L}[\mathcal{C}_{uj}] = CF(0) \tag{25}$$

where $CF(0)$ is the initial length of CF, $\mathcal{C}_{wi}$ and $\mathcal{C}_{uj}$ are the *ith* and *jth* wrapping and unwrapping evolutes, respectively, and $\mathcal{L}[\mathcal{C}_{wi}]$ and $\mathcal{L}[\mathcal{C}_{uj}]$ represent their lengths, respectively.

The existence of multiple solution trajectories is intuitive and is captured effectively in Remark 5 by the flexibility of the number and type of wrapping and unwrapping evolutes allowed for partial

reconfiguration. Additionally Eq. (25) represents a fundamental constraint for partial reconfiguration of the rolling sphere in planar geometry. The above condition can also be written as

$$\int_M \left\{ \hat{u}_t \cdot \frac{\overrightarrow{CF}}{|\overrightarrow{CF}|} \right\} ds = CF(0) \tag{26}$$

where $ds = |dx\hat{i} + dy\hat{j}|$, and M is the evolute and the path of integration. The flexibility in designing the evolute-involute pair while satisfying Eqs. (25) or (26) gives us the added freedom of posing a variety of optimization problems. For instance, we can define the partial reconfiguration problem as an isoperimetric problem [7], where the objective is to minimize the path length

$$J = \int_M ds \tag{27}$$

subject to the integral constraint in Eq. (26). From Eq. (7) we know that complete reconfiguration additionally requires convergence of β to zero. This requires the following integral condition to be satisfied:

$$\int_M \left(\frac{\partial \beta}{\partial r} \right) ds = -\beta_0 \tag{28}$$

where β_0 is the initial value of β. Eq. (26) alone, and together with Eq. (28), define the integral constraints for the isoperimetric problems for partial and complete reconfiguration, respectively. We do not solve the isoperimetric problem in this paper, instead we propose a class of solution trajectories that satisfy the integral constraints in Eqs. (26) and (28).

4 Partial Reconfiguration

In search of a class of solution trajectories for the problem posed in Sec. 3.2, we refer to the Sweep-Tuck algorithm in Sec. 2. With this algorithm, the sphere is reconfigured by a sequence of alternate circular arc and linear segments [6]. We will now show that under limiting conditions, the Sweep-Tuck algorithm yields a smooth trajectory of the sphere. Subsequently, we will establish that such a trajectory can be a solution for the problem posed by Eqs. (26) and (28).

4.1 Sweep-Tuck Algorithm With Smooth Motion. Consider the distance traversed by C during a DPT maneuver, as given in Eq. (17). For partial reconfiguration, we know that ψ must satisfy Eq. (13). As ψ approaches $\cos^{-1}(1/\lambda)$, we have

$$\lim_{\psi \to \cos^{-1}(1/\lambda)} CC' = \lim_{\psi \to \cos^{-1}(1/\lambda)} \frac{2\lambda CO(\lambda \cos\psi - 1)}{(\lambda^2 - 1)} = 0 \tag{29}$$

Also, from Eq. (15) we conclude that

$$\lim_{\psi \to \cos^{-1}(1/\lambda)} \psi' = \psi \tag{30}$$

From Definitions 1 and 2, we deduce that DPT and RS maneuvers become infinitesimally small and conclude that the points C and F, and hence the sphere, follow a smooth trajectory.

To corroborate the conclusion drawn above, we simulate the Sweep-Tuck algorithm for a general case and a case where $\psi \to \cos^{-1}(1/\lambda)$. The simulation results are shown in Figs. 8 and 9, respectively. Both simulations were performed with identical initial configuration of the sphere, given as follows:

$$(x\ y\ \theta\ \alpha\ \beta) = (7.0\ 1.0\ 1.4\ 0.5\ 2.5) \tag{31}$$

where the units are in meters and radians. The initial condition results in $\lambda = 1.684$, and the range of ψ in Eq. (13) to be $0 \leqslant \psi < \psi_{max} = \cos^{-1}(1/1.684) = 0.935$ rad. For the simulation in Fig. 8, ψ is chosen at 50% of ψ_{max} ($\psi_1 = 0.47$ rad), whereas, the choice of ψ is at 95% of ψ_{max} ($\psi_2 = 0.89$ rad) for the simulation in Fig. 9. In Figs. 8(a) and 9(a) the motion of F to F_1 is due to the PS and the first RS maneuver. The points F_1 mark the start of the first DPT maneuver. These points are shown by instances t_1 and t_2 in Figs. 8(c) and 9(c), respectively. Beyond these time instants C commences motion and θ starts decreasing due to the DPT maneuvers. The DPT maneuvers in Fig. 8(a) cause significant motion of the sphere but cause infinitesimal motion of the sphere in Fig. 9(a). This is evident in the motion of C which translates along the line

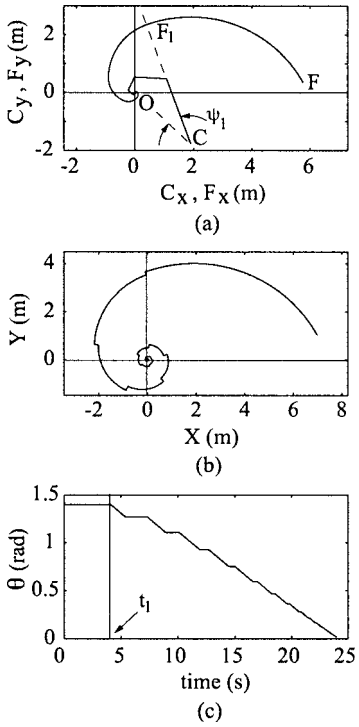

Fig. 8 Reconfiguration with $\psi < \cos^{-1}(1/\lambda)$

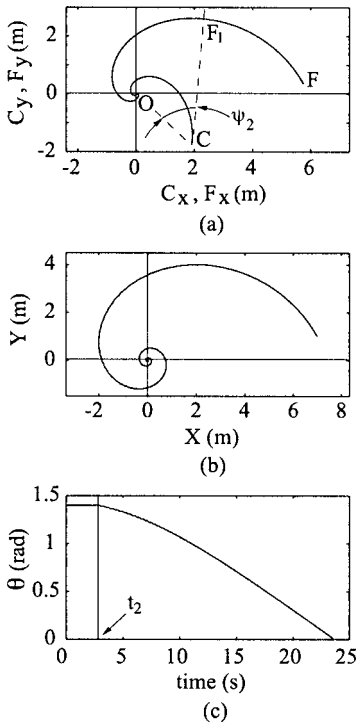

Fig. 9 Reconfiguration with $\psi \approx \cos^{-1}(1/\lambda)$

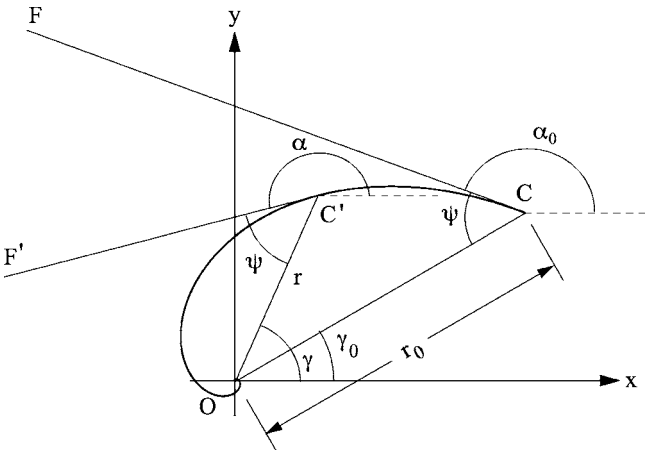

Fig. 10 A counterclockwise logarithmic spiral motion of *C*

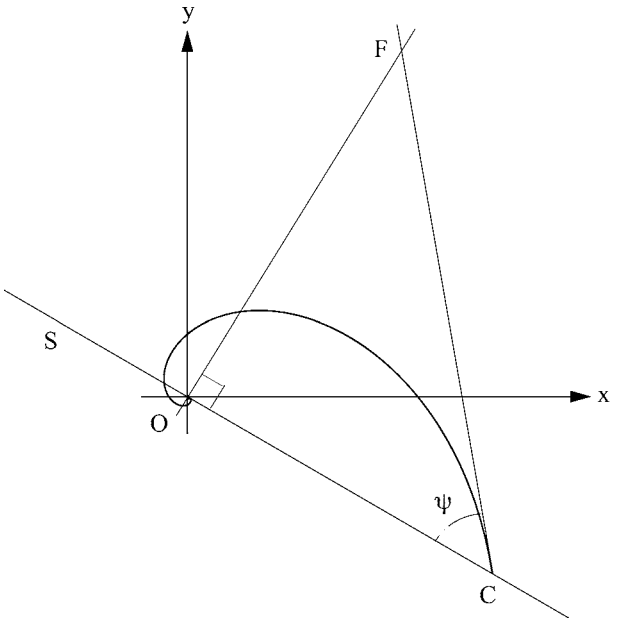

Fig. 11 Locus of *C* that allows partial reconfiguration

segments in Fig. 8(*a*), whereas in Fig. 9(*a*) it follows an almost smooth curve that is tangential to *CF*, thereby confirming Remark 4. It is clear from Fig. 8(*b*) and Fig. 9(*b*) that as ψ approaches $\cos^{-1}(1/\lambda)$, the trajectory of *C* and that of the sphere approach smooth curves. Also, θ decreases along a smooth curve in Fig. 9(*c*) whereas it decreases in alternate time intervals in Fig. 8(*c*).

4.2 Motion Along a Logarithmic Spiral. In a Sweep-Tuck sequence, both *CF* and *CO* decrease in geometric progression [6] at the end of every RS-DPT pair and finally converge to zero. As ψ approaches $\cos^{-1}(1/\lambda)$, the trajectory of *C* approaches a smooth curve with both *CF* and *CO* decreasing continuously to zero, as illustrated in Fig. 9(*a*). Since *CF* decreases, this smooth trajectory of *C* is a wrapping evolute curve according to Definition 4. Also, since Eq. (30) is satisfied, we deduce the following:

Remark 6. If the initial configuration of the sphere satisfies $\lambda \in (1,\infty)$, then, as ψ approaches the limiting value of $cos^{-1}(1/\lambda)$, the trajectory of the *C* generated by the Sweep-Tuck algorithm approaches a smooth wrapping evolute curve. Moreover, the tangent at any point on this curve makes a constant angle ψ with the radius vector $\vec{OC}$. Such a curve is the well known logarithmic spiral. Since any involute of a logarithmic spiral is also a logarithmic spiral [8], the trajectory of *F also approaches a logarithmic spiral motion*.

Consider a logarithmic spiral trajectory of the point *C* as shown in Fig. 10. The angle $\angle OC'F' = \psi$ is constant for any location *C* along its path and *r* represents the distance OC' which decreases with an increase in γ in this case. The spiral starts at $\gamma = \gamma_0$ where $r = r_0 = CO$. The mathematical expression of the logarithmic spiral can be derived easily from its definition, as

$$r = \begin{cases} r_0 e^{-(\gamma-\gamma_0)\cot\psi}, & \gamma_0 \leq \gamma < \infty \quad \text{for counter clockwise spiral} \\ r_0 e^{+(\gamma-\gamma_0)\cot\psi}, & -\infty < \gamma \leq \gamma_0 \quad \text{for clockwise spiral} \end{cases} \tag{32}$$

From Remark 6 it is evident that a logarithmic spiral is a potential solution to the geometric reconfiguration problem posed in Eq. (26). We will now establish that in the limiting case of $\psi = \cos^{-1}(1/\lambda)$, the length condition in Eq. (25) is satisfied. We consider a counterclockwise logarithmic spiral given in Eq. (32), the length of which can be computed using the expression

$$\mathcal{L}_C = \int_0^\infty \sqrt{r^2 + \left(\frac{dr}{d\gamma}\right)^2}\, d\gamma \tag{33}$$

where $\mathcal{L}_C$ is the length of the logarithmic spiral. Upon simplification, Eq. (33) yields

$$\mathcal{L}_C = \frac{r_0}{\cos\psi} = \frac{CO}{\cos\psi} = \lambda CO = CF \tag{34}$$

The same result is obtained upon considering a clockwise logarithmic spiral. This confirms that the logarithmic spiral satisfies Eq. (25) when $\psi = \cos^{-1}(1/\lambda)$ and is a solution trajectory of *C* for partial reconfiguration in the sense of Eq. (12). The choice of logarithmic spiral trajectory for the point *C*, the mathematical form in Eq. (32), and from the result above, we infer the following

Remark 7. A logarithmic spiral trajectory of *C*, converging to the origin, leads to exponential convergence of *CO* and *CF* to zero.

4.3 Partial Reconfiguration Using Logarithmic Spiral Motion of *C*. We concluded in Sec. 4.2 that the sphere can be partially reconfigured using a logarithmic spiral if the sphere configuration satisfies $\lambda \in (1,\infty)$ and $\angle OCF = \psi = \cos^{-1}(1/\lambda)$. Consider the second condition first

$$\cos\psi = (1/\lambda) \Rightarrow \cos\psi = \frac{CO}{CF} \Rightarrow FO \perp CO \tag{35}$$

An interesting observation here is that if *FO* is perpendicular to *CO*, then not only do we satisfy the second condition, but also the first condition. This is because

$$FO \perp CO \Rightarrow CF > CO \Rightarrow \lambda \in (1,\infty) \tag{36}$$

The result above implies that for a given point *F* defined by the initial conditions of the sphere, the point *C* should lie on a straight line perpendicular to *FO* and passing through *O* as shown in Fig. 11. Given *F*, the straight line *S* is the locus of the point *C* such that $FO \perp CO$ and $\cos\psi = 1/\lambda$. Therefore, for a given location of *F*, *S* is effectively the locus of the point *C* that allows the use of logarithmic spiral motion of *C* for partial reconfiguration.

We now devise a simple three step algorithm for achieving partial reconfiguration of the sphere from an arbitrary initial configuration. The three step algorithm is stated with the help of the next remark.

Remark 8. The rolling sphere can be partially reconfigured by the following three steps:

(1) Apply actuation (A) to make $\theta = 0$, i.e., make *C* and *F* coincident.

(2) Apply actuation (A) to move C to any point on the straight line that is perpendicular to FO and passing through O.
(3) Use logarithmic spiral motion of C with CF as the tangent to achieve partial reconfiguration.

The flexibility of choosing any point C along the line S will be utilized in the next section to achieve complete reconfiguration. We complete this section by deriving the expressions for the actuating inputs ω_x^1 and ω_y^1 that generate a logarithmic spiral motion of C. Differentiating the expression for x in Eq. (18) with respect to time, we have

$$\dot{x} = \dot{C}_x + \sec^2\theta \cos\alpha\dot{\theta} - \tan\theta \sin\alpha\dot{\alpha} \tag{37}$$

Considering a counterclockwise logarithmic spiral, from Fig. 10, C_x and $\dot{C}_x$ can be expressed as

$$C_x = r\cos\gamma \quad \dot{C}_x = -CO e^{-(\gamma-\gamma_0)\cot\psi}(\cot\psi\cos\gamma + \sin\gamma) \tag{38}$$

where the expression for r is given in Eq. (32) and CO is the initial distance of C from the origin. Here we assume $\dot{\gamma}=1 \equiv \gamma = t+\gamma_0$ without any loss of generality. To obtain the expressions for ω_x^1 and ω_y^1 we note from Fig. 10, that for a counterclockwise logarithmic spiral

$$\alpha = \pi - (\psi - \gamma) \Rightarrow \dot{\alpha} = \dot{\gamma} = 1 \tag{39}$$

Substituting Eqs. (1), (3), (4), and (38) into Eq. (37) and using Eq. (39), we obtain the following expressions for ω_y^1 and ω_x^1

$$\omega_y^1 = \frac{-CO}{\tan^2\theta \sin\psi} e^{-(\gamma-\gamma_0)\cot\psi}, \quad \omega_x^1 = -\tan\theta \tag{40}$$

Similar expressions can be deduced for a clockwise logarithmic spiral. Thus, the actuating inputs ω_x^1 and ω_y^1 that specifically generate a logarithmic spiral motion of C are smooth functions of time and the states of the system.

5 Complete Reconfiguration

From Fig. 11 it is evident that different choice of ψ in the second step of Remark 8 can result in different C along the locus S. When $\psi=\pi/2$, C coincides with O, and as ψ reduces to zero C moves farther away from O. We now show that the different logarithmic spirals generated due to the different end points C result in different $\Delta\beta$. Consider a counterclockwise logarithmic spiral given by Eq. (32). From Eqs. (33), (23), and (24), and Remark 5, we write

$$\Delta\mathcal{L} = \sqrt{r^2 + \left(\frac{dr}{d\gamma}\right)^2}\Delta\gamma = |\Delta CF| = -\tan^2\theta\Delta\theta \tag{41}$$

Rewriting Eq. (41) as

$$r_0 \csc\psi e^{-(\gamma-\gamma_0)\cot\psi} d\gamma = -\tan^2\theta d\theta \tag{42}$$

and integrating both sides of Eq. (42), we deduce the following:

$$e^{-(\gamma-\gamma_0)\cot\psi} = 1 - \frac{\cos\psi}{r_0}[(\tan\theta_0 - \theta_0) - (\tan\theta - \theta)] \tag{43}$$

Combining Eqs. (42) and (43) we have

$$d\gamma = -\frac{\tan^2\theta}{r_0\csc\psi - \cot\psi[(\tan\theta_0 - \theta_0) - (\tan\theta - \theta)]}d\theta \tag{44}$$

Also, from Eqs. (10), (39), and (44), we deduce the following:

$$d\alpha = d\gamma \Rightarrow d\beta = d\gamma(1-\sec\theta) \Rightarrow d\beta = \tan\psi\frac{\tan^2\theta(\sec\theta - 1)}{(\tan\theta - \theta)}d\theta \tag{45}$$

Thus, the total change in β due a counter clockwise logarithmic spiral motion of C can be given by the following expression

$$\Delta\beta = -\tan\psi\int_0^{\theta_0}\frac{\tan^2\theta(\sec\theta - 1)}{(\tan\theta - \theta)}d\theta \tag{46}$$

where, ψ is the constant angle $\angle OCF$ and θ_0 is the value of θ at the beginning of the logarithmic spiral motion of C. Consider the actuation (A) in second step of the algorithm presented in Remark 8 in Sec. 4.3. Using Fig. 11, ψ and θ_0 can be related by the expression

$$\frac{OF}{\sin\psi} = CF = \tan\theta_0 - \theta_0 \tag{47}$$

Clearly, different choices of ψ will result in different values of θ_0 in Eq. (47). As $\Delta\beta$ is a function of θ_0, Eq. (46), this in turn will yield different values of $\Delta\beta$. This is the key to complete reconfiguration of the sphere. From Fig. 11 clearly $0<\psi\leq\pi/2$. Also, from Eq. (47) we have

$$0 < \psi \leq \pi/2 \Rightarrow \pi/2 > \theta_0 \geq \bar{\theta}_0 \; \forall \; OF \neq 0 \tag{48}$$

where $(OF/\sin\psi)|_{\psi=\pi/2} = OF = \tan\bar{\theta}_0 - \bar{\theta}_0$. Note that, from Fig. 11 and Eq. (47), Eq. (46) can be rewritten as

$$\Delta\beta = -\frac{OF}{\sqrt{(\tan\theta_0 - \theta_0)^2 - OF^2}}\int_0^{\theta_0}\frac{\tan^2\theta(\sec\theta - 1)}{(\tan\theta - \theta)}d\theta \tag{49}$$

From the expression of $\Delta\beta$ in Eqs. (49) and (46), and from Eq. (48), one can deduce the following limits on $\Delta\beta$

$$\lim_{\theta_0\to\pi/2}\Delta\beta = -OF \Rightarrow \lim_{\psi\to 0}\Delta\beta = -OF$$

$$\lim_{\theta_0\to\bar{\theta}_0}\Delta\beta = -\infty \Rightarrow \lim_{\psi\to\pi/2}\Delta\beta = -\infty \tag{50}$$

It can be verified that the expression of $\Delta\beta$ in Eq. (49) is monotonic in θ_0. This leads to the following range of $\Delta\beta$;

$$0 < \psi \leq \pi/2 \Rightarrow \begin{cases} -OF \geq \Delta\beta > -\infty: & \text{counterclockwise logarithmic spiral} \\ OF \leq \Delta\beta < \infty: & \text{clockwise logarithmic spiral} \end{cases} \tag{51}$$

In Remark 8 note that β changes only during the logarithmic spiral motion in the third step and remains invariant during the first and second step of the partial reconfiguration algorithm. If β_0 is the initial value of β, then for complete reconfiguration,

$$\Delta\beta = -\beta_0 \tag{52}$$

Eq. (51) apparently puts a restriction based on the distance OF by imposing $-OF\leq\Delta\beta\leq OF$ to be an unachievable range of $\Delta\beta$. However, we can consider an equivalent β_0

$$\beta_{0\text{eq}} = \beta_0 \pm 2n\pi \tag{53}$$

where $n=1,2,\ldots$, such that the effective $\Delta\beta$, $\Delta\beta_{\text{eff}}$, given by

$$\Delta\beta_{\text{eff}} = -\beta_{0\text{eq}} \tag{54}$$

satisfies Eq. (51). This implies that any desired $\Delta\beta$ or its equivalent can be achieved, by appropriately choosing a point on the line S. Thus, while partial reconfiguration of the sphere can be achieved by following a logarithmic spiral trajectory of C starting from any point on the locus S as shown in Fig. 11, complete

reconfiguration in the sense of Eq. (7) can be achieved only from specific points on S. These points are such that the corresponding effective $\Delta\beta$ satisfies the relation

$$\Delta\beta_{\text{eff}} = \begin{cases} -\beta_{0eq}: & \Delta\beta \in (-OF, OF) \\ -\beta_0: & \Delta\beta \in (-\infty, -OF] \cup [OF, \infty) \end{cases} \tag{55}$$

We now modify our algorithm in Remark 8 to incorporate complete reconfiguration of the sphere as follows:

Remark 9. The rolling sphere can be completely reconfigured by applying the following three step algorithm:

(1) Apply actuation (A) to make $\theta=0$, i.e., make C and F coincident.
(2) Apply actuation (A) to move C to a point on the straight line S where $\psi = \angle OCF$ is such that $\Delta\beta_{\text{eff}}$ satisfies Eq. (55).
(3) Use logarithmic spiral motion of C with CF as the tangent to achieve complete reconfiguration.

We have defined the line S to be perpendicular to OF passing through the origin O. Consider the case when initial configuration of the algorithm makes F and O coincident. Then, the line OF degenerates to the origin and the line S is undefined. Although this is a special case of the algorithm, it can be handled easily. Consider first the case when F coincides with the origin but C does not. In this case we first apply an actuation (B) that causes O, C, and F to lie on a straight line and in that order. Subsequently, the complete reconfiguration algorithm in Remark 9 can be applied. Next consider the case when both C and F coincide with O. Then we first apply an actuation (A) to move C away from the origin. The rest follow exactly the same steps as the first case.

6 Simulations

In this section we show simulation results of the complete reconfiguration algorithm presented in Remark 9. The initial conditions of the sphere for this simulation are as follows:

$$(x\ y\ \theta\ \alpha\ \beta) \equiv (5\ 1.5\ 1.3\ -\pi/2\ -2.5) \tag{56}$$

where the units are in meters and radians. The initial conditions yield $OF=5.5036$ m, which implies that the minimum $|\Delta\beta|$ achievable is 5.5036 rad, whereas the necessary $\Delta\beta=2.5$ rad. Hence we consider an effective $\Delta\beta$ as follows:

$$|\Delta\beta_{\text{eff}}| = |2.5 + 2m\pi| > 5.5036 \text{ rad}, \quad \text{where } m = \pm 1, \pm 2, \ldots \tag{57}$$

We choose $m=1$ which yields $\Delta\beta=8.7832$ rad and an equivalent $\beta_{0_{\text{eq}}}=-8.7832$ rad. The simulation results are given in Fig. 12.

Figure 12(a) illustrates the C and F trajectories. The first step of the complete reconfiguration algorithm, Remark 9, where actuation (A) is applied, causes motion of C to C_1 which is coincident with F. In Fig. 12(c) this corresponds to the linear decrease of θ from 1.3 rad to zero at t_1. This is followed by the second step where actuation (A) takes C to C_2. In Fig. 12(c) this refers to the linear increase of θ from zero to 1.47 rad at t_2. The equivalent β remains constant at −8.7832 rad from $t=0$ to $t=t_2$. The point C_2 is such that $\angle C_2OF=\pi/2$ and this allows partial reconfiguration by a subsequent logarithmic spiral motion of C_2 to the origin. Also, with this choice of C_2, $\psi=\angle OC_2F=0.7019$ rad and the subsequent logarithmic spiral will cause $\Delta\beta=8.7832$ rad and thereby guarantee complete reconfiguration by additionally converging β to the origin. These initial maneuvers results in $\lambda=1.31$ (the algorithm guarantees that λ will necessarily be greater than 1). The subsequent logarithmic spiral motion converges C_2 and F simultaneously to the origin. The trajectories C_2O and FO form an evolute-involute pair. The resulting convergence of the sphere-center to the origin is shown in Fig. 12(b). The convergence of θ and β to the origin are illustrated in Figs. 12(c) and 12(d).

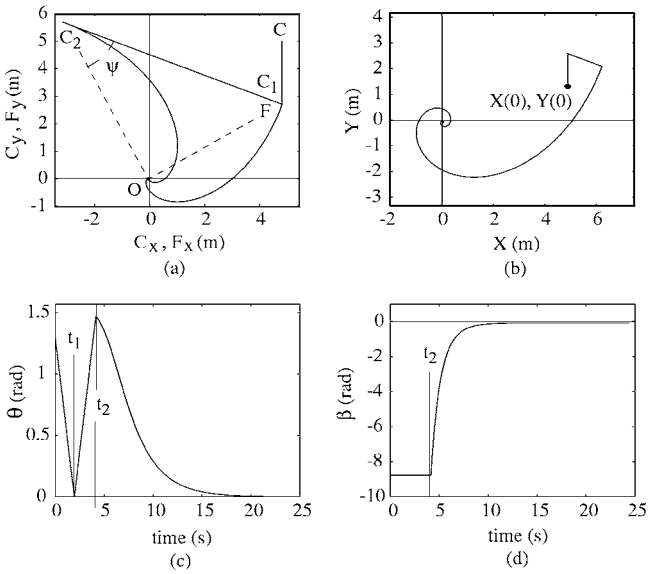

Fig. 12 Simulation showing complete reconfiguration using logarithmic spiral motion of *C*

7 Conclusion

In this paper we recast the classical problem of reconfiguration of a rolling sphere to a problem in planar geometry. We show that the rolling motion of a sphere is characterized by wrapping and unwrapping of a taut rope on a planar curve. The problem of reconfiguration therefore translates to that of designing an evolute-involute pair that originate at the initial configuration of the sphere and terminate at the desired configuration, while satisfying integral constraints. This geometric problem can be posed as an isoperimetric optimization problem, but rather than solving this problem directly, we obtain a class of solution trajectories where the evolute-involute pair are logarithmic spirals. It is shown that two preliminary maneuvers followed by a maneuver generated by the logarithmic spirals result in complete reconfiguration, and with exponential convergence of the configuration variables. We provide numerical simulations to illustrate the reconfiguration algorithm.

Acknowledgment

The authors gratefully acknowledge the support provided by National Science Foundation, NSF Grant No. CMS-9800343, in conducting this research.

References

[1] Hammersley, J., 1983, "Oxford Commemoration Ball," London Mathematical Society Lecture Notes, **79**, pp. 112–142.
[2] Li, Z., and Canny, J., 1990, "Motion of Two Rigid Bodies with Rolling Constraints," IEEE Trans. Rob. Autom., **6**(1), pp. 62–72.
[3] Jurdjevic, V., 1993, "The Geometry of the Plate-Ball Problem," Arch. Ration. Mech. Anal., **124**, pp. 305–328.
[4] Mukherjee, R., Minor, M., and Pukrushpan, J. T., 2002, "Motion Planning for a Spherical Mobile Robot: Revisiting the Classical Ball-Plate Problem," ASME J. Dyn. Syst., Meas., Control, **124**(4), pp. 502–511.
[5] Krener, A. J., and Nikitin, S., 1997, "Generalized Isoperimetric Problem," Journal of Mathematical Systems, Estimation, and Control, **7**(3), pp. 1–15.
[6] Das, T. , and Mukherjee, R., 2004, "Exponential Stabilization of the Rolling Sphere," Automatica, **40**, pp. 1877–1889.
[7] Courant, R., and Hilbert, D., 2003, *Methods of Mathematical Physics*, Wiley Interscience, New York, pp. 135–136.
[8] http://mathworld.wofram.com/Involute.html